

RTFusion: A depth estimation network based on multimodal fusion in challenging scenarios

Zelin Meng, and Takanori Fukao, *Member, IEEE*

Abstract— Depth estimation in complex real-world scenarios is a challenging task, especially when relying solely on a single modality such as visible light or thermal infrared (THR) imagery. This paper proposes a novel multimodal depth estimation model, RTFusion, which enhances depth estimation accuracy and robustness by integrating the complementary strengths of RGB and THR data. The RGB modality provides rich texture and color information, while the THR modality captures thermal patterns, ensuring stability under adverse lighting conditions such as extreme illumination. The model incorporates a unique fusion mechanism, EGFusion, consisting of the Mutual Complementary Attention (MCA) module for cross-modal feature alignment and the Edge Saliency Enhancement Module (ESEM) to improve edge detail preservation. Comprehensive experiments on the MS2 and ViViD++ datasets demonstrate that the proposed model consistently produces high-quality depth maps across various challenging environments, including nighttime, rainy, and high-glare conditions. The experimental results highlight the potential of the proposed method in applications requiring reliable depth estimation, such as autonomous driving, robotics, and augmented reality.

I. INTRODUCTION

Depth estimation is a fundamental yet challenging task in computer vision, playing a crucial role in applications such as autonomous driving, robotics, and augmented reality [1]. Accurate depth perception is essential for scene understanding, obstacle avoidance, and navigation. However, in real-world scenarios, particularly under challenging conditions such as nighttime, heavy rain, fog, or high-glare environments, depth estimation methods often struggle to maintain accuracy and robustness [2, 3].

Traditional approaches rely on single-modal inputs, primarily RGB images or thermal infrared (THR) imagery. RGB-based methods leverage rich texture and color information, making them well-suited for well-lit environments [4, 5]. However, their performance significantly deteriorates under low-light conditions or when visibility is obstructed. In contrast, THR-based methods capture heat signatures, enabling robust perception in dark or adverse weather conditions [6, 7]. Despite these advantages, THR images lack fine-grained texture details and high spatial resolution, leading to less precise depth predictions, particularly in geometrically complex scenes or low-contrast regions [8].

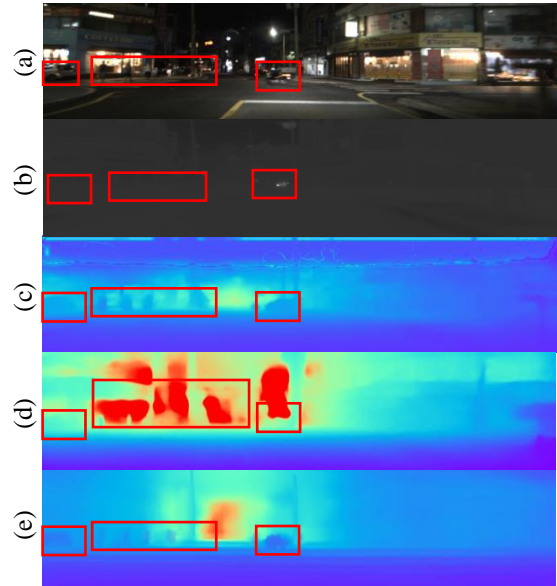


Figure 1. Predicted depth maps from different estimation Methods. (a): RGB input. (b): THR input. (c) Prediction from RGB-based method. (d): Prediction from THR-based method. (e): Prediction from RGB-THR fusion-based method.

Although both RGB and THR modalities have shown promising results, their standalone performance remains limited in challenging scenarios. To address this issue, multimodal fusion has emerged as a promising direction, aiming to combine the complementary strengths of RGB and THR data. RGB images provide detailed structural and color information, while THR images enhance robustness in low-visibility conditions by capturing thermal patterns [9, 10]. By integrating these modalities, multimodal depth estimation models have the potential to improve both accuracy and generalization across diverse environments [11].

Despite recent progress, several challenges remain in multimodal depth estimation [12, 13]. First, RGB and THR data exhibit inherent differences in spatial resolution, noise characteristics, and information distribution, making effective fusion difficult [14, 15]. Second, depth estimation in complex environments requires models to dynamically integrate global semantic information with fine-grained local details [15, 16]. Third, achieving scalable and adaptable multimodal fusion that

*Research supported by ABC Foundation.

F. A. Author is with the National Institute of Standards and Technology, Boulder, CO 80305 USA (corresponding author to provide phone: 303-555-5555; fax: 303-555-5555; e-mail: author@boulder.nist.gov).

S. B. Author, Jr., was with Rice University, Houston, TX 77005 USA. He is now with the Department of Physics, Colorado State University, Fort Collins, CO 80523 USA (e-mail: author@lamar.colostate.edu).

T. C. Author is with the Electrical Engineering Department, University of Colorado, Boulder, CO 80309 USA, on leave from the National Research Institute for Metals, Tsukuba, Japan (e-mail: author@nrim.go.jp).

generalizes well across different scenarios remains an open problem [17, 18].

In this work, we propose a novel multimodal depth estimation model designed to address these challenges. Our approach incorporates a cross-modal attention mechanism (MCA) and an Edge Saliency Enhancement Module (ESEM) to enhance RGB-THR feature fusion. By leveraging the complementary properties of both modalities, our method ensures robust and accurate depth estimation across a wide range of environmental conditions. Additionally, we introduce an edge enhancement module to refine depth predictions, particularly at object boundaries and in low-texture regions, further improving model performance in complex real-world scenarios. Our main contributions include the following:

1. We introduce a dual-branch feature extraction module tailored for RGB and THR (thermal infrared) data, independently modeling the characteristics of each modality. The RGB branch focuses on capturing texture details and global semantic information, while the THR branch enhances the perception of thermal radiation information, enabling better representation of temperature distributions in the scene.

2. To fully exploit the intrinsic complementarity between RGB and THR modalities, we introduce the Edge-Guided Fusion (EGFusion) module, comprising Mutual Complementary Attention (MCA) for cross-modal feature alignment and Edge Saliency Enhancement Module (ESEM) for structure-aware fusion. MCA leverages a Query-Key-Value mechanism to facilitate adaptive feature correspondence, enhancing cross-modal synergy and improving depth estimation in regions with severe occlusion and illumination variations. Meanwhile, ESEM enhances depth accuracy at object boundaries and in low-contrast regions by leveraging THR's temperature contrast advantage.

3. We conduct extensive experiments on the MS2 and VIVID++ datasets, achieving results significantly superior to current state-of-the-art single-modal and large-scale depth estimation models. Experimental results demonstrate that our method exhibits superior depth estimation performance in challenging scenarios such as low-light conditions, occlusions, and low-contrast regions.

II. RELATED WORK

Depth estimation methods can be broadly categorized into single-modality and multimodal approaches. Recent advancements in deep learning and self-supervised learning have significantly improved depth estimation accuracy, particularly in challenging environments [19].

A. Depth Estimation from RGB

Monocular depth estimation from RGB images has been extensively studied in computer vision. Traditional methods rely on handcrafted features and structure-from-motion techniques, while recent advances leverage deep learning to extract depth information from single images. Vision transformers (ViTs) have been introduced for dense prediction tasks, replacing convolutional networks to improve depth estimation accuracy by utilizing global receptive fields. Similarly, large models like "Depth Anything" focus on scaling up the dataset to improve generalization and zero-shot capabilities, significantly enhancing depth estimation

performance on public benchmarks [12]. Laplacian pyramid-based methods have also been proposed to refine depth estimation by preserving multi-scale depth residuals, improving both boundary sharpness and global consistency [16]. Self-supervised approaches further mitigate the need for labeled depth data by employing photometric consistency constraints, leading to state-of-the-art results in various datasets, including KITTI and NYUv2 [9, 25].

RGB-based depth estimation utilizes rich texture and color information but suffers from sensitivity to lighting variations and occlusions [25, 28]. In contrast, THR-based methods leverage thermal signatures for robustness in low-light conditions but lack spatial resolution and texture details. Recent advances, including unsupervised domain adaptation and self-supervised learning, aim to enhance single-modality depth estimation by improving generalization and reducing domain shifts [26].

B. Depth Estimation from THR

On the other hand, thermal infrared (THR)-based approaches offer a distinct advantage by capturing heat signatures, making them robust to lighting changes. These methods are particularly effective in scenarios where visible light is limited, such as during nighttime or in foggy conditions. Recent methods have been developed to estimate depth and ego-motion from thermal images by leveraging multi-spectral consistency losses [7]. Additionally, techniques like adversarial multi-spectral adaptation use unpaired RGB-THR images to improve feature extraction and depth prediction for thermal inputs [20]. Some works propose direct depth estimation from single thermal images by incorporating generative adversarial networks (GANs) and contour-aware constraints, which help mitigate the lack of texture in thermal images. Large-scale multi-spectral stereo datasets have also been created to benchmark depth estimation models under various lighting and weather conditions, aiding in the development of more robust thermal-based depth estimation techniques [27].

However, THR imagery lacks the detailed texture and fine-grained information available in RGB data, often leading to less precise depth maps, especially in scenes with complex geometries or low thermal contrast. As a result, THR-based methods are somehow insufficient for robust depth estimation across diverse environments.

C. Depth Estimation from Fused RGB and THR

Fusing RGB and THR modalities enhances depth estimation by leveraging the strengths of both domains. RGB provides rich texture and semantic information, while THR ensures robust performance in low-visibility environments. Multi-modal fusion frameworks have been proposed to integrate dominant depth cues from both sources using confidence-based fusion networks [25]. Some methods employ cross-modality transformers to enhance feature interaction between RGB and THR, improving depth prediction accuracy in complex scenarios [26]. Additionally, self-supervised learning frameworks have been designed to exploit multi-spectral image pairs, ensuring better depth generalization across varying environments [27]. A novel approach, "MURF," integrates image registration and fusion to correct parallax errors while extracting aligned multi-modal

depth representations, further improving depth estimation performance [29].

Recent approaches integrate RGB and THR data to leverage RGB’s texture details and THR’s thermal stability, addressing single-modality limitations. While early fusion methods concatenate features directly, they often suffer from redundancy and conflicts. Advanced strategies, such as mid-level and late fusion, use attention models, gated fusion, or feature alignment to enhance complementarity [29, 30]. However, scalability and feature alignment remain challenges. To address these issues, our method employs hierarchical multi-scale fusion with Mutual Complementary Attention (MCA) for effective RGB-THR integration and an Edge Saliency Enhancement Module (ESEM) to refine depth predictions, improving robustness and accuracy in complex environments.

III. PROPOSED METHOD

A. Model Architecture

The proposed model employs a modular architecture tailored for effective multimodal fusion. It consists of three primary components: feature extraction, feature fusion, and decoding.

Feature Extraction. Independent feature extraction branches are designed for RGB and THR modalities. The RGB branch employs an optimized ConvNeXt Tiny architecture to capture detailed texture, edge, and color information. Conversely, the THR branch focuses on extracting thermal gradients and edge features specific to thermal data. Both branches incorporate a hierarchical multi-scale structure, progressively capturing fine-grained local details and global context. This modular design ensures that modality-specific characteristics are preserved, enabling optimal feature extraction for subsequent fusion.

We are given an RGB image and a THR (thermal cameras) image, and the network outputs the expected depth map. The input data is defined as follows:

$$X^{RGB} \in \mathbb{R}^{3 \times H \times W}, X^{THR} \in \mathbb{R}^{1 \times H \times W} \quad (1)$$

The RGB and THR images are separately fed into two ConvNeXt Tiny backbone networks with non-shared parameters.

$$F_{RGB}^l, F_{RGB}^h = \text{ConvNeXtTiny}_{RGB}(x^{RGB}) \quad (2)$$

$$F_{THR}^l, F_{THR}^h = \text{ConvNeXtTiny}_{THR}(x^{THR}) \quad (3)$$

Here, F_{RGB}^l and F_{RGB}^h denote the low-level and high-level feature representations extracted from the RGB modality, F_{THR}^l, F_{THR}^h correspond to the low-level and high-level feature representations derived from the THR modality.

Then, we upsample the features from the THR modality to align them with those from the RGB modality and subsequently incorporate learnable positional embeddings to capture spatial dependencies.

$$\tilde{F}_{THR}^l = \text{Interp}(F_{THR}^l) \quad (4)$$

$$\tilde{F}_{THR}^h = \text{Interp}(F_{THR}^h) \quad (5)$$

B. Feature Fusion

To fully exploit the complementary properties of RGB and THR modalities, we propose the Edge-Guided Fusion (EGFusion) module, which consists of two key components: Mutual Complementary Attention (MCA) for cross-modal feature alignment, and Edge Saliency Enhancement Module (ESEM) for structure-aware fusion.

For the low-level feature, the process is defined as follows:

$$F_{fused}^l = \text{EGFusion}(F_{RGB}^l, F_{THR}^l) \quad (6)$$

Specifically, the EGFusion operation can be explained as the following process.

Add learnable position embeddings to capture spatial dependencies:

$$\hat{F}_{RGB}^l = F_{RGB}^l + PE, \hat{F}_{THR}^l = \tilde{F}_{THR}^l + PE \quad (7)$$

$$\hat{F}_{RGB}^h = F_{RGB}^h + PE, \hat{F}_{THR}^h = \tilde{F}_{THR}^h + PE \quad (8)$$

At this stage, the superscript $\hat{}$ denotes features with position encoding applied, while PE represents the position encoding itself.

Mutual Complementary Attention (MCA). To effectively capture the complementary relationships between RGB and THR modalities, we design a Mutual Complementary Attention (MCA) mechanism based on a Query-Key-Value (QKV) structure, enabling dynamic interaction between the two modalities. Given the input RGB and THR features, we first extract attention components and to reduce computational complexity and enlarge the receptive field, we apply a 3×3 convolution with stride $s = 2$ for downsampling:

$$Q^l = \text{Conv}_{1 \times 1}(F_{RGB}^l), \bar{Q}^l = \text{Conv}_{3 \times 3}^{s=2}(Q^l) \quad (9)$$

$$K^l, V^l = \text{Conv}_{1 \times 1}(\tilde{F}_{THR}^l), \bar{K}^l, \bar{V}^l = \text{Conv}_{3 \times 3}^{s=2}(K^l, V^l) \quad (10)$$

Where Q^l is extracted from F_{RGB}^l via a 1×1 convolution, while K^l, V^l are obtained from \tilde{F}_{THR}^l using the same 1×1 convolution operation. To reduce computational complexity and enlarge the receptive field, the downsampled representations $\bar{Q}^l, \bar{K}^l, \bar{V}^l$ are obtained through a 3×3 convolution with a stride of $s = 2$.

The attention weights and output are computed:

$$A^l = \text{softmax}\left(\frac{\bar{Q}^l \bar{K}^l}{\sqrt{d_k}}\right) \quad (11)$$

Here, $\sqrt{d_k}$ serves as a scaling factor to prevent excessively large values that could lead to gradient vanishing. The attention weights A^l are applied to the Value to compute the weighted sum:

$$O^l = A^l \bar{V}^l \quad (12)$$

Since the attention computation is performed on the downsampled features, we apply an upsampling operation to restore the original resolution:

$$\hat{O}^l = \text{Interp}(O^l) \quad (13)$$

Where *Interp* denotes bilinear interpolation.

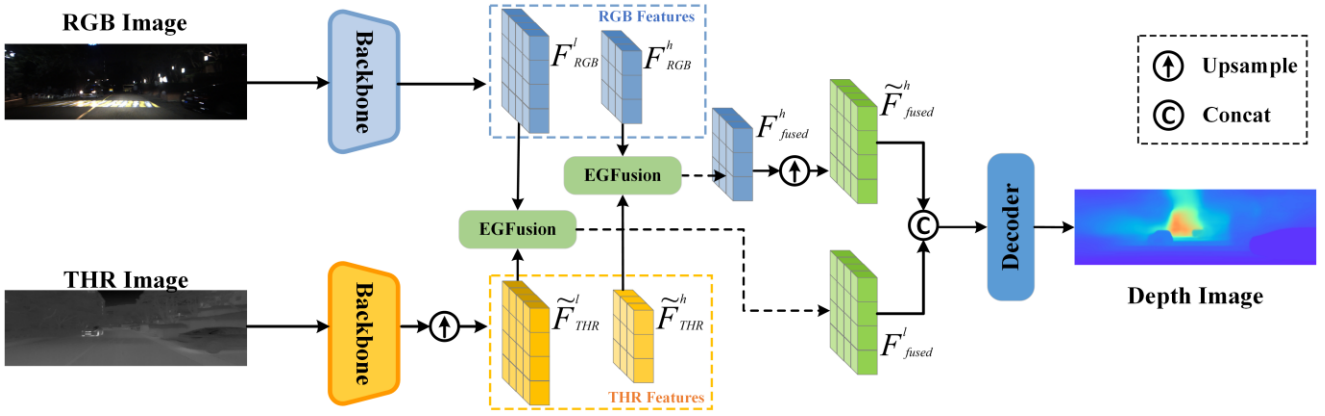


Figure 1. Overall architecture of the RTFusion depth estimation networks.

Finally, the RGB features enhanced by cross-modal attention are defined as follows:

$$F_{cross}^l = \hat{F}_{RGB}^l + \tilde{O}^l \quad (14)$$

Edge Saliency Enhancement Module (ESEM). The computation process of ESEM is formulated as:

$$F_{enhanced}^l = \text{ESEM}(F_{THR}^l, F_{cross}^l) \quad (15)$$

Where the input F_{THR}^l is the low-scale feature extracted from the THR modality. F_{cross}^l is the cross-attention RGB feature obtained from MCA.

Specifically, ESEM can be defined as follows:

First, an edge weight map E^l is computed by applying a two-layer convolutional network to the thermal feature map \hat{F}_{THR}^l :

$$E^l = \sigma(\mathbf{W}_2 \cdot \text{ReLU}(\mathbf{W}_1 \cdot \hat{F}_{THR}^l)) \quad (16)$$

$$F_{enhanced}^l = F_{cross}^l + E^l \odot \hat{F}_{THR}^l \quad (17)$$

Here, E^l represents the learned edge weight map, which is generated by applying a two-layer convolutional network parameterized by \mathbf{W}_1 and \mathbf{W}_2 , both of which are learnable parameters. Specifically, \mathbf{W}_1 is a 3×3 convolutional kernel that extracts local structural features and enhances edge-related information, while \mathbf{W}_2 is a 1×1 convolutional kernel responsible for aggregating channel-wise information and reducing dimensionality to produce a single-channel edge weight map. The output is further refined through a non-linear activation function, where ReLU enhances feature discrimination after \mathbf{W}_1 , and Sigmoid normalizes the final response to the range $[0,1]$, ensuring its suitability for edge-aware fusion. The edge-aware weighting mechanism leverages the thermal gradient information to adaptively adjust the contribution of THR features in the fused representation. High values of E^l indicate strong edge presence, where thermal information is crucial for preserving object boundaries. In such regions, THR features are emphasized to enhance structural details. Conversely, lower values of E^l suppress the contribution of THR information in homogeneous regions,

preventing irrelevant thermal noise from affecting the RGB features. This ensures that the fusion process is guided by

meaningful structural cues rather than indiscriminate feature blending.

Next, we employ convolutional layers to further integrate the cross-modal features:

$$F_{fused}^l = \text{FusionConv}(F_{enhanced}^l) \quad (18)$$

After obtaining the F_{fused}^l , we apply the same operations to the high-level features. Consequently, we derive the high-scale fused feature representation, denoted as F_{fused}^h .

After aligning the high-level and low-level features using bilinear interpolation, the feature fusion is performed:

$$F_{concat} = \text{Concat}(F_{fused}^l, \text{Interp}(F_{fused}^h)) \quad (19)$$

C. Decoding Mechanism

The decoding stage reconstructs high-resolution depth maps from the fused features. A multi-stage upsampling architecture progressively refines depth predictions, integrating hierarchical features from earlier stages to preserve both detail and consistency, ensuring accurate and realistic depth reconstructions. The decoder is employed to generate the final depth estimation:

$$D = \text{UNetDecoder}(F_{concat}) \quad (20)$$

Where D represents the output depth map.

D. Loss Function

The $L1$ loss minimizes the absolute error between the predicted depth map and the ground truth. This ensures that the overall structure of the scene is accurately captured, reducing large deviations in predicted depth values:

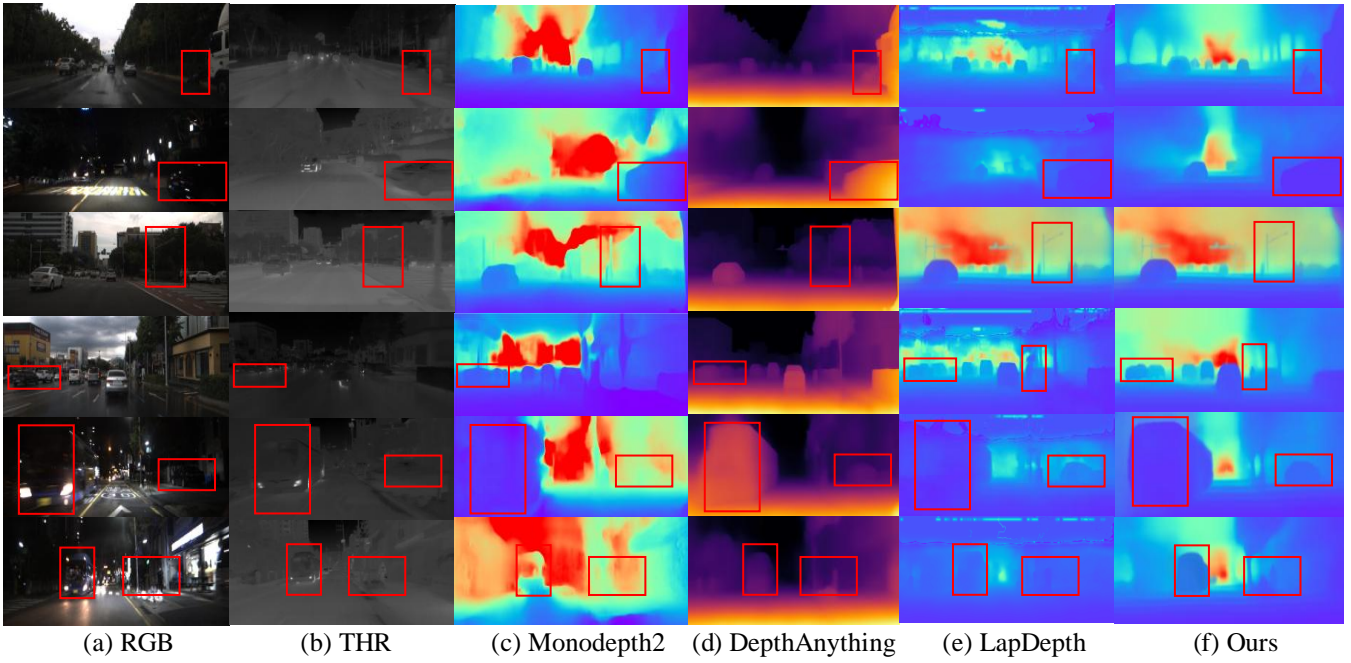


Figure 3. Qualitative results of different depth estimation methods. First column: RGB inputs. Second column: THR inputs. Third column: results from Monodepth [24]. Forth column: results from large model [12]. Fifth column: results from LapDepth [16] Sixth column: results from the proposed method RTFusion.

$$L_{L1} = \frac{1}{N} \sum |D_{pred}(i) - D_{gt}(i)| \quad (21)$$

where N is the total number of pixels, and i indexes the pixel locations.

To enhance the accuracy of depth predictions at object boundaries, an edge-preserving smoothness term is introduced. This term penalizes large depth variations in non-edge regions while preserving sharp transitions at edges. The edge-preserving smoothness loss is defined as:

$$L_{smooth} = \sum_i |\nabla D_{pred}(i)| \cdot \exp(-|\nabla I(i)|) \quad (22)$$

where ∇D_{pred} represents the depth gradient, ∇I is the image intensity gradient from the RGB modality, and the exponential term reduces the penalty near high-gradient (edge) regions.

The final loss function combines the $L1$ loss and the edge-preserving smoothness loss to achieve a balance between global accuracy and boundary refinement:

$$L_{total} = \lambda_1 L_{L1} + \lambda_2 L_{smooth} \quad (23)$$

where λ_1 and λ_2 are weighting factors that control the contribution of each loss component. These parameters are tuned to ensure that the model optimizes both accuracy and edge precision effectively.

IV. EXPERIMENTAL RESULTS

A. Dataset and Setup

The MS2 dataset (Multi-Spectral 2) is a dataset designed to contain pairs of RGB (visible light) and thermal (infrared) images, often used for research in areas such as object detection, tracking, and scene recognition under different

environmental conditions. The dataset is typically utilized in multi-modal machine learning tasks, where models need to process and integrate information from both visible and thermal images.

The dataset includes synchronized RGB and thermal images captured by specialized cameras. Thermal images provide information that is not visible in the RGB spectrum, such as heat signatures from objects or individuals. The dataset includes images captured in a variety of environmental conditions and scenarios. This can include outdoor settings, indoor environments, and nighttime captures where thermal imaging provides critical information not available in RGB images. Since thermal imaging can provide unique insights, it is often used in conjunction with RGB data to enhance object detection, especially under poor lighting conditions or challenging environments (e.g., night, fog, or rain).

The proposed model was evaluated on multiple publicly available MS2 datasets to ensure comprehensive testing across diverse environmental conditions. The datasets included scenes captured during daytime, nighttime, and under challenging conditions such as fog, rain, and glare. These scenarios provided a robust testbed for evaluating the multimodal fusion approach.

The RGB and THR images were preprocessed to ensure alignment and scale consistency. Data augmentation techniques, including random cropping, flipping, and brightness adjustment, were applied to improve generalization capability of the model. The evaluation metrics used include root mean squared error (RMSE), etc.

B. Evaluation Metrics

The evaluation metrics used for quantitative evaluation are defined as follows:

TABLE I. QUANTITATIVE EVALUATIONS OF DEPTH ESTIMATION RESULTS ON THE MS2 DATASET

Method		Modality	Metrics						
			AbsRel↓	SqRel↓	RMSE↓	RMSE(log)↓	$a_1 \uparrow$	$a_2 \uparrow$	$a_3 \uparrow$
MSFT [20]	2022	THR	0.128	1.264	5.691	0.266	0.821	0.919	0.965
BTS [9]	2019	THR	0.129	1.008	5.169	0.206	0.843	0.947	0.978
MTVUMCL [27]	2021	THR	0.155	1.367	5.944	0.280	0.811	0.917	0.963
MS2 (Stereo) [7]	2023	THR	0.120	1.057	<u>5.068</u>	0.207	0.872	0.949	0.975
LapDepth [16]	2021	RGB	0.125	1.054	5.394	0.223	0.853	0.944	0.979
MIM [23]	2023	RGB	0.124	1.102	5.283	0.216	0.855	0.940	0.970
AFNet [28]	2024	RGB	0.122	1.093	5.214	0.220	0.866	0.947	0.973
MCT [30]	2023	THR+RGB	<u>0.116</u>	<u>1.015</u>	5.192	<u>0.202</u>	<u>0.884</u>	<u>0.951</u>	<u>0.980</u>
MURF [29]	2023	THR+RGB	0.121	1.062	5.124	0.210	0.869	0.948	0.973
RTFusion (Ours)		THR+RGB	0.104	0.942	4.997	0.186	0.895	0.974	0.991

$$AbsRel = \frac{1}{N} \sum_{i=1}^N \left| \frac{y_i - y_i^{pred}}{y_i} \right| \quad (24)$$

$$SqRel = \frac{1}{N} \sum_{i=1}^N \left(\frac{y_i - y_i^{pred}}{y_i} \right)^2 \quad (25)$$

$$RMSE = \sqrt{\frac{1}{N} \sum_{i=1}^N (y_i - y_i^{pred})^2} \quad (26)$$

$$RMSE(log) = \sqrt{\frac{1}{N} \sum_{i=1}^N (\log((y_i + 1) - \log(y_i^{pred} + 1)))^2} \quad (27)$$

Where N denotes the total number of pixels with ground truth labels in the depth map. y_i indicates the ground truth depth value and y_i^{pred} represents predicted depth value for i_{th} pixel. The RMSE measures the average magnitude of the error between predicted and actual depth values. The AbsRel metric measures the mean of the absolute relative errors. The SqRel metric measures the mean of the squared relative errors. Besides, we also adopt delta metrics to verify the performance of our proposed methods. In specific, for each pixel p , compute the ratio as follows:

$$r(p) = \min\left(\frac{\hat{D}(p)}{D(p)}, \frac{D(p)}{\hat{D}(p)}\right) \quad (28)$$

consistently achieve better results than single-modal methods that rely solely on RGB or THR.

In addition to quantitative evaluations, we conducted a visual comparison (Figure 1), showing that traditional RGB-based methods struggle in low-light conditions, often producing blurred depth maps. In contrast, RTFusion effectively integrates RGB and THR data, achieving clearer and more accurate depth predictions, particularly in challenging regions. The Edge Saliency Enhancement Module (ESEM) refines depth edges by leveraging THR’s temperature contrast, reducing blurring and discontinuities. Additionally, the Mutual Complementary Attention (MCA) mechanism enhances depth estimation in occluded and low-contrast areas, ensuring smoother and more reliable predictions.

Then, we count the number of pixels where $r(p) < 1.25$ for δ_1 , $r(p) < 1.25^2$ for δ_2 , $r(p) < 1.25^3$ for δ_3 , respectively. Finally, we divide these counts by the total number of pixels to get the percentage of pixels meeting the criteria for each metric.

C. Experiment Results

In this study, extensive experiments were conducted on the MS2 and ViViD++ datasets to compare the proposed RTFusion method with state-of-the-art single-modal and multi-modal depth estimation approaches. The results demonstrate that our method achieves superior performance across multiple evaluation metrics.

Tables 1 and 2 present the experimental results on the MS2 and ViViD++ datasets, respectively. As shown in the results, the proposed RTFusion method outperforms other approaches in key metrics such as AbsRel, SqRel, and RMSE. Specifically, on the MS2 dataset, our method achieves an RMSE of 4.997, significantly surpassing MCT (5.192) and MURF (5.124). Furthermore, on the ViViD++ dataset, our method attains an AbsRel of 0.052, outperforming MCT (0.060) and MURF (0.066). These findings indicate that RTFusion enables more accurate scene depth reconstruction, particularly in complex environments. In addition, as observed in Tables 1 and 2, multi-modal fusion methods based on RGB and THR

D. Ablation Studies

Multimodal Fusion Strategy. To further validate the effectiveness of multimodal fusion in the proposed RTFusion method, we conducted additional experiments on the MS2 dataset to analyze the performance of different approaches across various scenarios, including daytime, nighttime, and rainy conditions. The detailed experimental results are presented in Table 3, where RGB denotes the use of only RGB image data within the original RTFusion framework (i.e., without the THR branch), and THR represents the use of only THR image data (i.e., without the RGB branch).

As shown in Table 3, the proposed multimodal fusion depth estimation method consistently achieves the best performance across all scenarios, with particularly notable improvements in nighttime and rainy conditions. For example,

in terms of the AbsRel metric, RTFusion reduces the error by 0.045 compared to the RGB single-modal approach and by 0.009 compared to the THR single-modal approach in nighttime scenarios. In rainy conditions, RTFusion achieves an error reduction of 0.008 compared to the RGB single-modal method and 0.015 compared to the THR single-modal method.

Additionally, an analysis of Table 3 reveals that THR outperforms RGB significantly in nighttime scenarios, likely due to the superior capability of thermal cameras in capturing scene features under low-light conditions. In summary, these experimental results suggest that the proposed multimodal fusion strategy offers advantages in handling challenging environments, such as adverse weather and poor lighting conditions.

TABLE II. ABLATION STUDY ON PROPOSED ESEM MODULE

Module	AbsRel↓	SqRel↓	RMSE↓	$\alpha_1 \uparrow$
Without Enhancement	0.119	1.055	5.228	0.869
Sobel-based	0.111	1.014	5.083	0.891
Canny-based	0.115	1.018	5.175	0.887
ESEM (ours)	0.104	0.942	4.997	0.895

TABLE III. ABLATION STUDY ON PROPOSED FUSION METHOD

Module	AbsRel↓	SqRel↓	RMSE↓	$\alpha_1 \uparrow$
Concat	0.121	1.075	5.226	0.868
SENet	0.112	1.004	5.056	0.891
Transformer	0.114	1.009	5.098	0.889
Ours	0.104	0.942	4.997	0.895

To assess the contributions of individual components within the proposed model, ablation studies were conducted by removing the cross-modal attention mechanism (MCA), the edge saliency enhancement module (ESEM), and their effects on depth estimation performance were analyzed.

Mutual Complementary Attention. The MCA dynamically matches RGB and THR features to fully exploit their complementary advantages. When this mechanism was removed, AbsRel increased from 0.104 to 0.121, and RMSE rose to 5.226. These results indicate that MCA effectively enhances cross-modal feature interaction, thereby improving depth estimation accuracy.

Edge Saliency Enhancement Module. The ESEM module leverages the temperature contrast advantage of THR data to enhance depth prediction accuracy at object boundaries. When ESEM was removed, RMSE increased from 4.997 to 5.228, and AbsRel rose to 0.119. Further analysis of depth maps revealed noticeable blurring at object boundaries, demonstrating the importance of ESEM for boundary refinement.

Through comparison and ablation experiments, our method has demonstrated significant advantages in depth estimation tasks. The cross-modal attention mechanism effectively fuses RGB and THR features, the edge saliency enhancement module refines depth prediction at object boundaries. The synergy of these components enables our

method to provide high-quality depth estimation results across various complex environments.

V. CONCLUSION

The proposed multimodal fusion depth estimation model demonstrates superior performance by leveraging the complementary strength of RGB and THR data. Its innovative architecture and loss design enable accurate and robust depth estimation across diverse scenarios, making it a valuable tool for complex real-world applications.

REFERENCES

- [1] Zhu J, Liu L, Jiang B, "Self-supervised Event-based Monocular Depth Estimation using Cross-modal Consistency," IEEE/RSJ International Conference on Intelligent Robots and Systems (IROS), 2023, pp. 7704-7710.
- [2] Zhang T, Zhu D, Zhang G, "Spatiotemporally Enhanced Photometric Loss for Self-Supervised Monocular Depth Estimation," IEEE/RSJ International Conference on Intelligent Robots and Systems (IROS), 2022, pp. 01-08.
- [3] Lo S Y, Wang W, Thomas J, "Learning feature decomposition for domain adaptive monocular depth estimation," IEEE/RSJ International Conference on Intelligent Robots and Systems (IROS), 2022, pp. 8376-8382.
- [4] Fraser H, Wang S, "Monocular Depth Estimation for Equirectangular Videos," IEEE/RSJ International Conference on Intelligent Robots and Systems (IROS), pp. 5293-5299, 2022.
- [5] Hirose N, Tahara K, "Depth360: Self-supervised Learning for Monocular Depth Estimation using Learnable Camera Distortion Model," IEEE/RSJ International Conference on Intelligent Robots and Systems (IROS), 2022, pp. 317-324.
- [6] Wu D, Zhu D, Zhang G, "J-RR: Joint Monocular Depth Estimation and Semantic Edge Detection Exploiting Reciprocal Relations," IEEE/RSJ International Conference on Intelligent Robots and Systems (IROS), 2022, pp. 715-722.
- [7] Shin U, Park J, Kweon I S, "Deep depth estimation from thermal image," Proceedings of the IEEE/CVF Conference on Computer Vision and Pattern Recognition, 2023, pp. 1043-1053.
- [8] Lee A J, Cho Y, Shin Y, "ViViD++: Vision for visibility dataset," IEEE Robotics and Automation Letters, vol. 7, pp. 6282-6289, 2022.
- [9] Lee J H, Han M K, Ko D W, "From big to small: Multi-scale local planar guidance for monocular depth estimation," arXiv preprint arXiv:1907.10326, 2019.
- [10] Qin Z, Xu J, Zhao W, "Adaptive Stereo Depth Estimation with Multi-Spectral Images Across All Lighting Conditions," arXiv preprint arXiv:2411.03638, 2024.
- [11] Fu H, Gong M, Wang C, "Deep ordinal regression network for monocular depth estimation," Proceedings of the IEEE Conference on Computer Vision and Pattern Recognition, 2018, pp. 2002-2011.
- [12] Yang L, Kang B, Huang Z, "Depth anything: Unleashing the power of large-scale unlabeled data," Proceedings of the IEEE/CVF Conference on Computer Vision and Pattern Recognition, 2024, pp. 10371-10381.
- [13] Ranftl R, Bochkovskiy A, Koltun V, "Vision transformers for dense prediction," Proceedings of the IEEE/CVF International Conference on Computer Vision. 2021: 12179-12188.
- [14] Vankadari M, Hodgson S, "Dusk till dawn: Self-supervised nighttime stereo depth estimation using visual foundation models," IEEE International Conference on Robotics and Automation (ICRA), 2024, pp. 17976-17982.
- [15] Gil, Hyeonjae, Myung-Hwan Jeon, and Ayoung Kim, "Fieldscale: Locality-aware field-based adaptive rescaling for thermal infrared image," IEEE Robotics and Automation Letters, 2024.
- [16] Song M, Lim S, Kim W, "Monocular depth estimation using laplacian pyramid-based depth residuals," IEEE transactions on Circuits and Systems for Video Technology, vol.31(11), pp. 4381-4393, 2021.
- [17] Li J, Wang P, Xiong P, "Practical stereo matching via cascaded recurrent network with adaptive correlation," Proceedings of the

- IEEE/CVF Conference on Computer Vision and Pattern Recognition, pp. 16263-16272, 2022.
- [18] Lu Y, Lu G, "An alternative of lidar in nighttime: Unsupervised depth estimation based on single thermal image," Proceedings of the IEEE/CVF Winter Conference on Applications of Computer Vision, pp. 3833-3843, 2021.
 - [19] Ke, Bingxin, Obukhov A, et al, "Repurposing diffusion-based image generators for monocular depth estimation," Proceedings of the IEEE/CVF Conference on Computer Vision and Pattern Recognition, 2024.
 - [20] Shin, Ukcheol, "Maximizing self-supervision from thermal image for effective self-supervised learning of depth and ego-motion," IEEE Robotics and Automation Letters, vol. 7(3), pp. 7771-7778, 2022.
 - [21] Shin, Ukcheol, et al, "Self-supervised depth and ego-motion estimation for monocular thermal video using multi-spectral consistency loss," IEEE Robotics and Automation Letters, vol.7(2), pp. 1103-1110, 2021.
 - [22] Shin, Ukcheol, et al, "Self-supervised monocular depth estimation from thermal images via adversarial multi-spectral adaptation," Proceedings of the IEEE/CVF Winter Conference on Applications of Computer Vision, 2023.
 - [23] Xie, Zhenda, et al, "Revealing the dark secrets of masked image modeling," Proceedings of the IEEE/CVF Conference on Computer Vision and Pattern Recognition, 2023.
 - [24] Godard C, Mac Aodha O, Firman M, et al, "Digging into self-supervised monocular depth estimation," Proceedings of the IEEE/CVF International Conference on Computer Vision, pp. 3828-3838, 2019.
 - [25] Guo Y, Qi X, Xie J, "Unsupervised cross-spectrum depth estimation by visible-light and thermal cameras," IEEE Transactions on Intelligent Transportation Systems, vol. 24(10), pp. 10937-10947, 2023.
 - [26] Xu J, Liu X, Jiang J, et al, "Unveiling the depths: A multi-modal fusion framework for challenging scenarios," arXiv preprint arXiv:2402.11826, 2024.
 - [27] Shin, Ukcheol, et al, "Self-supervised depth and ego-motion estimation for monocular thermal video using multi-spectral consistency loss," IEEE Robotics and Automation Letters, vol. 7(2), pp. 1103-1110, 2021.
 - [28] Cheng Junda, et al, "Adaptive fusion of single-view and multi-view depth for autonomous driving," Proceedings of the IEEE/CVF Conference on Computer Vision and Pattern Recognition, 2024.
 - [29] Xu Ha, Jiteng Yuan, and Jiayi Ma, "Murf: Mutually reinforcing multi-modal image registration and fusion," IEEE Transactions on Pattern Analysis and Machine Intelligence, vol. 45(10), pp. 12148-12166, 2023.
 - [30] Wang X, Wang X, Song R, et al, "MCT-Net: Multi-hierarchical cross transformer for hyperspectral and multispectral image fusion," Knowledge-Based Systems, vol. 264, pp. 110362, 2023.